



Validation of an individualized home-made superficial brachytherapy mold applied for deep nonmelanoma skin cancer

Ramin Jaber^{1,2}, Zahra Siavashpour³, Naser Zare Akha¹, Mohammad Hadi Gholami⁴, Fatemeh Jafari¹, Mandana Biniaz⁵

¹Cancer Institute, Tehran University of Medical Science, Yas Hospital, Tehran, Iran

²Department of Physics, University of Surrey, Guildford, United Kingdom

³Department of Radiotherapy Oncology, Shohada-e Tajrish Educational Hospital, Medical School, Shahid Beheshti University of Medical Sciences, Tehran, Iran

⁴Department of Medical Radiation Engineering, Science and Research Branch, Islamic Azad University, Tehran, Iran

⁵Department of Radiation Oncology, Hamedan University of Medical Sciences, Hamedan, Iran

ABSTRACT

Background: This study was conducted to evaluate the effect of brachytherapy (BT) customized mold [Condensation silicone elastomer (Protesil™)] and its thickness on the dose distribution pattern of deep nonmelanoma skin cancers (NMSC).

Materials and methods: Four blocks of mold material were constructed in 5, 10, 15, and 20 mm thickness and 100 × 100 mm² area by a plastic cast. The high dose rate (HDR) plus treatment planning system (TPS) (Version 3, Eckert & Ziegler BEBIG GmbH, Berlin, Germany) with a ⁶⁰Co source (model: Co0.A86, EZAG BEBIG, Berlin, Germany) as an high dose rate brachytherapy (HDR-BT) source was used. Solid phantom and MOSFET™ and GAFCHROMIC™ EBT3 film dosimeters were used for experimental dosimetry of the different thicknesses (up to 20 mm) of BT customized mold. Skin dose and dose to different depths were evaluated.

Result: The TPS overestimated the calculated dose to the surface. Skin dose can be reduced from 250% to 150% of the prescription dose by increasing mold thickness from 5 mm to 20 mm. There was a 7.7% difference in the calculated dose by TPS and the measured dose by MOSFET. There was a good agreement between film dosimetry, MOSFET detector, and TPS' results in depths less than 5 mm.

Conclusion: Each BT department should validate any individualized material chosen to construct the customized surface BT mold. Increasing the mold thickness can treat lesions without overexposing the skin surface. Superficial BT can be recommended as an appropriate treatment option for some deep NMSC lesions (up to 20 mm) with pre-planning considerations employing thicker molds.

Key words: HDR-BT; mold; nonmelanoma skin cancer; dosimetry

Rep Pract Oncol Radiother 2022;27(6):1010-1018

Address for correspondence: Zahra Siavashpour, Department of Radiotherapy Oncology, Shohada-e Tajrish Medical Center, School of Medicine, Shahid Beheshti University of Medical Science, Tehran, Iran, tel: (0098) 9120298176; e-mail: z_siavashpour@sbmu.ac.ir, zahrasiavashpour@gmail.com

This article is available in open access under Creative Common Attribution-Non-Commercial-No Derivatives 4.0 International (CC BY-NC-ND 4.0) license, allowing to download articles and share them with others as long as they credit the authors and the publisher, but without permission to change them in any way or use them commercially

Introduction

Nonmelanoma skin cancer (NMSC) is the most common malignancy worldwide, and its incidence has an increasing trend as the population gets older [1–3]. The two most frequent NMSCs are basal cell carcinoma (BCC) and squamous cell carcinoma (SCC). Although NMSC has a low morbidity and mortality rate, it can significantly affect the patient's quality of life [1].

Among cancer treatment options, including surgery, radiotherapy, photodynamic therapy, and chemotherapy [4], radiation therapy has an essential role in managing NMSC [5]. Superficial, ortho/megavoltage X-rays, electron beam irradiation, and radionuclide-based brachytherapy (BT) are various radiotherapy modalities applied to NMSC. High dose rate brachytherapy (HDR-BT) is a technique that supplies a high dose rate of a low-energy x-ray in the tumor area with minimal shielding requirement [6–9]. Because of the widespread availability of HDR-BT, it has become a powerful option for radiotherapy, particularly for clinical cases where surface irregularity, bone proximity, or poor inherent tolerance of surrounding tissues do not allow for suitable dose distribution [10]. Merkel cell lesions, keloids, and Kaposi sarcoma are the other kinds of skin cancer that HDR brachytherapy can be considered an alternative solution [10].

Due to the dose distribution of EBRT and its commercial applicators, surface mold brachytherapy, in addition to 3D treatment planning based on CT images, has emerged as an appropriate option in the treatment planning of organs like the head and neck [11]. Also, shielded cup-shaped applicators are restricted to lesions of less than 3 cm in diameter for both ValenciaTM and Leipzig [12]. For larger lesions, catheter flaps such as the FreiburgTM flap, Catheter Flap SetTM, H.A.M.TM, or individualized routine-made molds are widely used [13]. At our institution, an individualized home-made surface mold has been used to BT of widespread NMSC that cannot be excised surgically or for irregular-shaped lesions.

AAPM TG-43 is the most common code of practice used for most dose calculations in clinical brachytherapy. TG-43 protocol estimates dose distributions in water, is strictly valid for homogeneous water medium and does not consider the actual inhomogeneity around the BT source [14, 15]. Some

new model-based dose calculation algorithms, such as advanced collapsed cones, have been presented to enhance treatment planning systems (TPS) that can be considered full scatter condition inhomogeneity medium [12]. Nowadays, many treatment planning systems still use TG-43 basic protocols. It has been recently shown that the delivered dose can be up to 15% lower at the prescription depth than that considered by the TG-43 model for surface mold HDR brachytherapy. This difference increased with the skin lesion size [16]. Consequently, before their employment in clinical practice, some dosimetry and quality control examinations should be evaluated and approved for individualized routine-made molds, mainly when just TG-43-based TPSs are presented.

High dose gradient and rapid dose fall-off are the intrinsic characteristics of brachytherapy dose distribution that require particular radiation detectors to provide proper and accurate dose calculations. The most common radiation detection systems used for dose measurements in brachytherapy are thermoluminescent dosimeters (TLDs), radiochromic film detectors, and metal-oxide semiconductor field-effect transistors (MOSFETs) [17]. TLD and film detectors are inexpensive and commonly accessible in radiotherapy departments, but they are offline, and also their calibration procedure is a vital problem. MOSFETs can be considered credible miniature detectors for online in vivo dosimetry and quality assurance (QA) [18].

This study was conducted to confirm a mold BT procedure in our institute and examine whether the delivered dose to the tissue agrees with TG-43 protocols when a customized mold material is used. Therefore, three main aims were followed; (a) comparing the skin HDR-BT delivered dose to the patient obtained from experimental dosimetry setups and calculating dose with TPS, (b) investigating the optimum individualized molds thickness according to different thicknesses and depth of target lesions and, finally, (c) acquisition of the maximum lesion thickness that can be treated with the suggested BT mold. This study was specially conducted to evaluate the effect of a home-made brachytherapy (BT) customized mold (Condensation silicone elastomer (ProtesilTM) thickness on the dose distribution pattern of deep non-melanoma skin cancers (NMSC). MOSFETTM

and GAFCHROMICTM EBT3 film dosimetry as two reliable brachytherapy dosimeters were used for following the mentioned aims.

Materials and methods

Condensation silicone elastomer material with the commercial name Protesil™ (Vannini Dental Industry, Florence, Italy) is used in dentistry as a common material to shape a surface mold. These materials are classified as a group of elastomeric impressions with suitable physical and chemical properties such as biocompatibility, sufficient working time, room temperature working condition, dimensional stability, plasticity, non-toxicity, and electron density [19].

The HDR plus treatment planning system (Version 3, Eckert & Ziegler BEBIG GmbH, Berlin, Germany) with the dose calculation algorithm extensively detailed at AAPM Task Group-43 (TG-43) as a brachytherapy TPS was used. MultiSource™ (Eckert & Ziegler BEBIG GmbH, Berlin, Germany) as HDR-BT afterloader treatment unit, and a ⁶⁰Co radioactive source (model: Co0.A86, EZAG BEBIG, Berlin, Germany) as an HDR-BT source, was also applied. Dose verification measurements were performed using Gafchromic EBT3 film (Ashland Specialty Ingredients, NJ, USA lot#09071703 and #04171901) and three MOSFET™ detectors to be described in the following section. Previous researchers confirmed the feasibility and efficiency of MOSFET detectors in real-time in-vivo dosimetry for brachytherapy [20, 21].

Mold construction

Four blocks of mold material were constructed in 5, 10, 15, and 20 mm thickness and 100 × 100 mm² area by a plastic cast. The mold was removed from the cast after 15 to 20 minutes. Three plastic catheters (Flexible Catheter Single Leader, 1.65 mm

diameter, Eckert & Ziegler BEBIG, GmbH, Berlin, Germany) were fixed on top of each mold block via adhesive tape and with 10 mm parallel spacing between the catheters.

MOSFET calibration

In the current study, the MOSFET dosimeters (Best Medical Canada LTD model TN-502RD-H) with a sensitive volume of fewer than 4×10^{-5} mm³ and a physical volume of 4 mm³ were utilized. The MOSFET Calibration Jig (TN-RD-57-30, Best Medical Canada) was applied to the facile and reproducible placement of the MOSFETs through calibration and measurement. The jig is an accessory of the mobile MOSFET wireless patient dosimetry system (TN-RD-70-W, Best Medical Canada) [22]. MOSFET detectors were placed on the surface of the jig, with the flat surface facing the beam during all the experimental measurements.

PMMA slabs were also used in the calibration step; 10 cm of slabs were located under the detectors to provide the backscatter condition, and 2 cm of slabs were placed on the MOSFET for buildup effect. The calibration was carried out for a field size of 10 × 10 cm² with an SSD of 98 cm (100 cm at the MOSFET plane). The MOSFETs were then irradiated with 100 cGy by a 6 MV photon beam with a mono-energy medical linear accelerator (Compact, Elekta, Veenendaal, the Netherlands), and the corresponding readings were tabulated in Table 1.

MOSFETs were initially positioned in the jig channels, as all of them were placed into a 100 × 100 mm² central square. The first detector was in the center (red arrow), the second was in the upper right (10 mm to the right and 10 mm up from the center; yellow arrow), and the third one was in the lower left (10 mm to the left and 10 mm down from the center; blue arrow); as illustrated in Supplementary File as Figure S1.

Table 1. Calibration results of metal–oxide semiconductor field-effect transistors (MOSFETs)

MOSFET	Blue	Red	Yellow	Mean ± SD	Blue	Red	Yellow	Mean ± SD
	[cGy/mV]				[cGy/mV]			
	First step				Second step			
1	1.03	1.01	1.05	1.03 ± 0.02	1.04	1.03	1.06	1.04 ± 0.01
2	1.02	1.01	1.03	1.02 ± 0.01	1.03	1.01	1.05	1.03 ± 0.02
3	1.00	1.00	1.01	1.00 ± 0.01	1.01	1.00	1.03	1.01 ± 0.01

SD — standard deviation

CT simulation and dose calculations

A 64-slice CT scanner (General Electric Medical Systems, USA) was also applied to acquire tomographic imaging to provide data required to be imported to the TPS. CTIs were acquired with 1 mm slice thickness. Metallic x-ray markers were also placed inside the catheters during scanning.

Two configurations of source loading for comparing the TPS data with MOSFET dose calculations were performed. Details of the procedure are briefly explained in the sections below.

Setup 1: The central point of the central BT catheter located just above the central MOSFET detector at the middle of the jig, shown as red MOSFET in Supplementary File — Figure S1, was activated. The planning aim was to deliver 3 Gy to 10 mm under the phantom surface, the XZ plane of the central point. Eventually, four treatment plans were performed for four mold thicknesses, with the identical prescribed dose to the same point of interest.

Twenty-four setup configurations were created using a combination of 30 cm PMMA slabs. The radiation doses were then calculated for 6 points at different depths for four different mold thicknesses. More details of the configurations are shown in Figure 1. At this step, 72 dose points (24 setups \times 3 MOSFET) were compared for various mold thicknesses by the MOSFET.

Setup 2: A treatment plan was developed to deliver a 3 Gy radiation dose to all three MOSFETs. Radiation doses into a point located at 10 mm under the skin for different mold thicknesses were measured using MOSFET detectors. All measurements were repeated three times for all configurations. The processed results were then compared with those calculated by TPS. The Source to Detector Distance (SDD) was defined as follows:

$$SDD = \frac{t_{catheter}}{2} + t_{slab} + t_{mould} + \frac{t_{MOSFET}}{2}$$

Where $t_{catheter}$, t_{mold} , t_{slab} , and t_{MOSFET} are the measured thicknesses of the catheters, the mold, the PMMA slab, and the MOSFET detector, respectively. The SDD was used to calculate the depth of the intended plane in TPS-calculated 3D dose distribution and coincide with the MOSFET plane to define the exact position of control points in TPS.

It should be emphasized that to prevent the angular dependency of the MOSFET detector, the direction of entrance radiation to the MOSFET at all of the calculations set up were set to be the same as the calibration condition.

Film dosimetry

A calibration curve was obtained with eight pieces of $2 \times 2 \text{ cm}^2$ GAFCHROMIC™ EBT3 films, shown in Supplementary File — Figure S2, to ver-

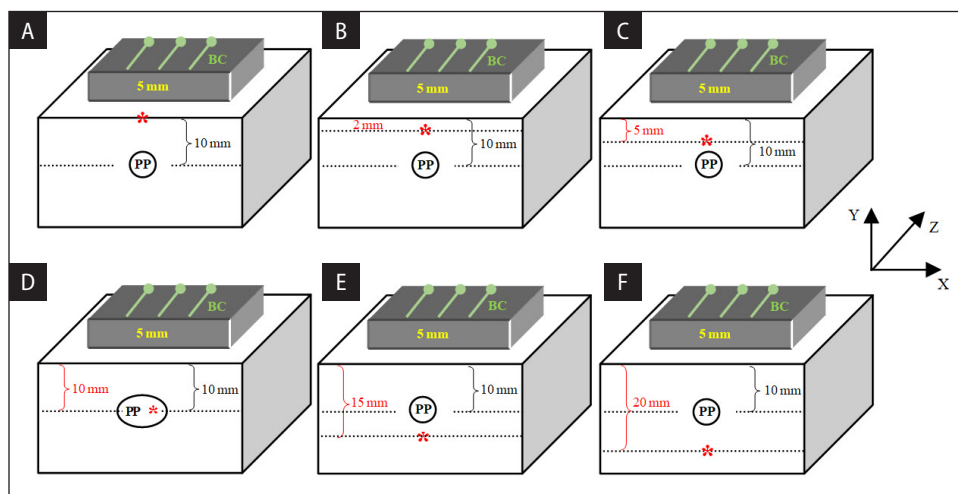


Figure 1. Set up the configuration for a mold with 5 mm thickness positioned on the top of a 30 cm PMMA slab. Measurements were done at the (A) surface, (B) 2 mm, (C) 5 mm, (D) 10 mm, (E) 15 mm, and (F) 20 mm depths (shown in red star) while the dose prescribed to a central point (shown as PP) at a depth of 10 mm

ify the film response to irradiation with the dose range from 1 to 9 Gy. For calibration curve measurements, buildup conditions and background radiation were also taken into consideration. Film dosimetry was performed for all four mold thicknesses explained at 2–3–1. An EBT3 film (5 × 10 mm) slice was also positioned under the mold surface.

Results

MOSFET calibration

As mentioned in the method, calibration factors (CF) of MOSFETs were calculated. When MOSFETs were exposed to a 6 MV photon beam, the CF factors were discovered to be in the range of 1.00 to 1.05 cGy/mV. Table 1 represents the MOSFET results after 1 Gy exposure.

Dose calculation

Results of the Setup 1 configuration, represented in section 2-3-1, to compare the calculated dose in TPS and MOSFET are presented in Figure 2. Based on this figure results, skin dose reduces approximately from 250% (about 7.5 Gy) to 150% (about 5 Gy) of the prescription dose at the red MOSFET. Therefore, using mold thickness from 5 mm to 20 mm reduces skin dose significantly.

The results of the Setup 2 configuration, which was performed by treatment planning aimed to de-

liver a 3 Gy to all the three MOSFETs, are presented in Table 2.

Film dosimetry

The calibration curve of the GAFCHROMIC™ EBT3 film was drawn in Supplementary File — Figure S3.

Discussion

Many particular and routine applicators are dedicated to BT of skin in clinical practice, such as Valencia, Leipzig, and even electronic BT applicators verified for NMSC [11]. However, these applicators' compatibility with any non-uniformity of skin types is restricted. Applying personalized home-made surface mold is a common approach in brachytherapy [11, 13, 23, 24].

The significant benefit of such modified mold construction is reaching the best shape conformity to the various curvatures of body sites. For instance, Budrukkar et al. reported using a dental acrylic mold in HDR-BT for head and neck tumors and concluded that this therapy has excellent organ preservation functions [23]. We used condensation silicone elastomer material to construct our individualized skin BT mold. Based on the current study results, this material with the commercial name Protesil™ can be used to make an individualized superficial BT mold.

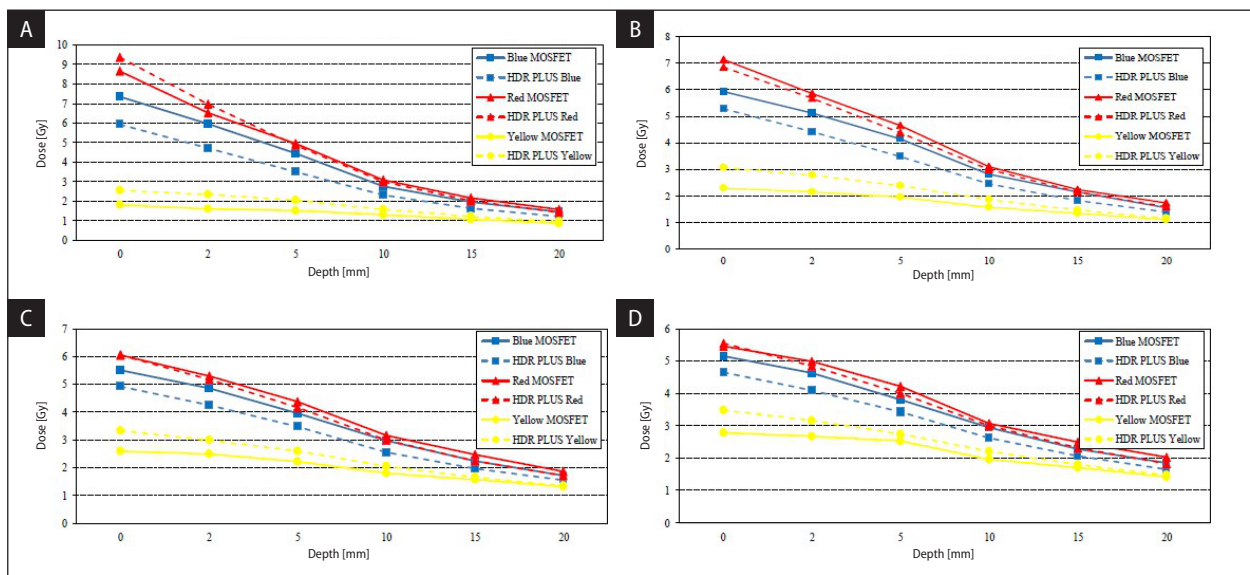


Figure 2. Calculated dose for (A): 5 mm (B): 10 mm (C): 15 mm (D): 20 mm mold thickness during deferent depths from the surface of the phantom

Table 2. Comparing metal–oxide semiconductor field-effect transistors (MOSFETs) measured and treatment planning systems (TPS) calculated doses for the setup 2 configuration to deliver a 3 Gy to all the three MOSFETs

Molds Thickness	MOSFET Color	Readings (cGy)				
		1	2	3	Mean ± SD	Difference ± SD
5 mm	Blue	317	314	314	315 ± 1.7	4.9 ± 0.5
	Red	307	312	303	307 ± 4.5	2.5 ± 1.6
	Yellow	316	323	318	319 ± 3.6	6.4 ± 1.2
10 mm	Blue	320	316	321	319 ± 2.6	6.4 ± 0.9
	Red	322	319	321	321 ± 1.5	6.9 ± 0.6
	Yellow	314	319	317	317 ± 2.5	5.5 ± 0.7
15 mm	Blue	310	312	317	313 ± 3.6	4.2 ± 1.2
	Red	317	315	316	316 ± 1.0	5.3 ± 0.4
	Yellow	324	320	322	322 ± 2.0	7.4 ± 0.7
20 mm	Blue	309	317	308	311 ± 4.9	3.9 ± 1.7
	Red	310	309	307	309 ± 1.5	3.0 ± 0.5
	Yellow	318	314	319	317 ± 2.6	5.6 ± 0.9

SD — standard deviation

MOSFET detectors have good indications to be used for dosimetry of high dose gradient regions due to their small sensitive volumes, which can result in high spatial resolution data for accurate dosimetry. Moreover, MOSFET dosimeters are online and independent of dose rate. Melchert et al. used MOSFET for online in vivo dosimetry during interstitial brachytherapy of thoracic-wall, head and neck, and breast cases [21]. In another study, Persson et al. applied MOSFET to perform an end-to-end ^{192}Ir quality assurance (QA) procedure. After dose verification measurements, they figured out the stability of MOSFET detectors over time and their good functionality for QA in brachytherapy [25].

Due to the previous studies, reaching an unsuccessfully full scatter condition is a fundamental problem in superficial brachytherapy, which leads to systematic uncertainty, about 5%, especially within the first 5 mm of the skin surface [26]. Therefore, the discrepancy in dosage measured by MOSFETs (shown by the red arrow in Supplementary File — Fig. S1) at distances less than 5 mm from the phantom surface from the TPS results is acceptable.

The TPS and MOSFET output differences were higher for blue and yellow MOSFET detectors in less than or equal to 5 mm depth. These two MOSFETs were not at the same XY plane (Fig. 1), and due to rapid dose fall in small SDD, higher

alterations were predictable. After 10 mm for all of the mold thicknesses, the differences between MOSFETs and TPS output were negligible (less than 0.1 Gy). Melchert et al. also concluded that the deviations between TPS results and measured dose were influenced by the proximity of their detectors to the target [21]. Our results agree with their conclusion, particularly for the high dose region that occurred in-depth below 5 mm from the phantom surfaces.

The other noticeable results that can be seen in Figure 2 are for the BT mold with 5 mm thickness, for which the TPS calculated dose was 7.7% higher than the MOSFET detector result (red) at the surface of the phantom. It can be concluded that TG-43-based TPSs overestimated the dose at the surface by considering the mold's material as water. This point should be taken into consideration when we are facing patients with unhealed lesions after surgery. Beyond 2 mm from the surface, this difference became insignificant (Fig. 2A). This difference cannot be generalized to the thicker molds. By increasing mold thickness, data matching between the central MOSFET and TPS outputs was improved.

Considering Figures 4A–D, the inverse square law effect was observed. Increasing the mold thickness, the dose per plane of the prescription point (i.e., 10 mm in this study) became higher. Doses at the 15 and 20 mm depths were higher when

we applied molds with 15 and 20 mm thickness. However, due to the attenuation effect of phantom and mold, by increasing the thickness of mold by more than 20 mm, no more dose escalation was observed.

Table 2 represents the experimental results of all three MOSFETs at the prescription dose. The differences between the calculated dose with TPS and peripheral MOSFET detectors are found to be identical with the central MOSFET, as expected. The maximum difference between the MOSFET's data and the TPS outputs was 7.4 ± 0.7 %. By considering the results, we can conclude that the sensitivity of the MOSFET to the exposure angle did not influence their reading in the current study.

EBT3 film, due to its near tissue-equivalent characteristic and independent energy range, is suitable for BT with a ^{60}Co source for a dose of more than 100 cGy [26]. Furthermore, any positional inaccuracy between source and film causes significant inaccuracy in final achievements. As shown in Supplementary File — Figure S4, loss of scattering equilibrium or any positional uncertainty leads to a difference of up to 35% between the calculated dose in film and TPS at the surface of the phantom. Several studies used EBT2 or EBT3 films as dosimeters in various BT dosimetry procedures [27–30]. Sinnantamby et al. performed a verification study to evaluate the radiation dosimetry in HDR-BT by EBT2 film. They used several film stacks to confirm the AcurosTMBV algorithm and applied this detector to make the quality assurance of cylinder applicators with/without the shield but with a buildup cap of 5 mm or thicker. Gamma analysis of their results demonstrated the reliability of the QA procedure, particularly with 5% and 1 mm [29]. Bassi et al. used EBT3-V3 film for dosimetry assessment of a 3D printable material in surface BT as a mold. Their results were in good agreement with Oncentra Brachy TPS when two films were irradiated at 5 mm and 15 mm distance from their 3D-printed 5 mm slab [27]. However, due to the high dose gradient, there is no report for dosimetry data in a distance less than 5 mm near the BT source.

Figure S4 in Supplementary File demonstrates that the positioning uncertainties are inversely proportional to the SSD, especially for film studies. The relative difference between film data and the TPS results is reduced to 4% in 20 mm

under the skin. On the surface of the phantom, the results of film dosimetry were unreliable. Beyond 5 mm, all the film, MOSFET, and TPS calculated doses are in good agreement with each other.

HDR-BT of NMSC with individualized skin molds cause conformal radiotherapy with a high biologically equivalent dose, advanced functional outcomes, and high local control of tumor [24]. However, any BT center must validate its customized mold material.

Conclusion

Based on the present study results, each BT department should validate any individualized material chosen to construct the customized surface BT mold. Moreover, the MOSFET detector can be employed as a reliable online dosimeter in NMSC superficial BT. TPS calculation of the dose distributions based on the TG-43 algorithm would overestimate the skin dose through superficial BT. Furthermore, film dosimetry would cause unreliable outputs for HDR superficial BT. Increasing the mold thickness by more than 20 mm depth allows deep NMSC lesions to be treated without overexposing the skin. Therefore, superficial BT can be used as a treatment option for NMSC lesions that are even thicker than 5 mm, but more than 20 mm deep.

Ethical permission

Ethical approval was not necessary for the preparation of this article.

Acknowledgements

The authors would like to express their deepest gratitude to the radiotherapy department of the Yas Hospital, Tehran, Iran, for supporting the irradiations.

Conflicts of interest

None declared.

Funding

None declared.

References

1. Lomas A, Leonardi-Bee J, Bath-Hextall F. A systematic review of worldwide incidence of nonmelanoma skin cancer. *Br J Dermatol.* 2012; 166(5): 1069–1080,

- doi: [10.1111/j.1365-2133.2012.10830.x](https://doi.org/10.1111/j.1365-2133.2012.10830.x), indexed in Pubmed: [22251204](https://pubmed.ncbi.nlm.nih.gov/22251204/).
2. Perera E, Ganeswaran N, Staines C, et al. Incidence and prevalence of non-melanoma skin cancer in Australia: A systematic review. *Australas J Dermatol*. 2015; 56(4): 258–267, doi: [10.1111/ajd.12282](https://doi.org/10.1111/ajd.12282), indexed in Pubmed: [25716064](https://pubmed.ncbi.nlm.nih.gov/25716064/).
 3. Veness MJ, Delishaj D, Barnes EA, et al. Current Role of Radiotherapy in Non-melanoma Skin Cancer. *Clin Oncol (R Coll Radiol)*. 2019; 31(11): 749–758, doi: [10.1016/j.clon.2019.08.004](https://doi.org/10.1016/j.clon.2019.08.004), indexed in Pubmed: [31447088](https://pubmed.ncbi.nlm.nih.gov/31447088/).
 4. Treatments for non-melanoma skin cancer. <https://www.cancer.ca/en/cancer-information/cancer-type/skin-non-melanoma/treatment/?region=on>.
 5. Ouhib Z, Kasper M, Perez Calatayud J, et al. Aspects of dosimetry and clinical practice of skin brachytherapy: The American Brachytherapy Society working group report. *Brachytherapy*. 2015; 14(6): 840–858, doi: [10.1016/j.brachy.2015.06.005](https://doi.org/10.1016/j.brachy.2015.06.005), indexed in Pubmed: [26319367](https://pubmed.ncbi.nlm.nih.gov/26319367/).
 6. Conill C, Sánchez-Reyes A, Molla M, et al. Brachytherapy with 192Ir as treatment of carcinoma of the tarsal structure of the eyelid. *Int J Radiat Oncol Biol Phys*. 2004; 59(5): 1326–1329, doi: [10.1016/j.ijrobp.2004.01.048](https://doi.org/10.1016/j.ijrobp.2004.01.048), indexed in Pubmed: [15275716](https://pubmed.ncbi.nlm.nih.gov/15275716/).
 7. Shields JA, Shields CL, Freire JE, et al. Plaque radiotherapy for selected orbital malignancies: preliminary observations: the 2002 Montgomery Lecture, part 2. *Ophthalmic Plast Reconstr Surg*. 2003; 19(2): 91–95, doi: [10.1097/01.IOP.0000056020.66654.33](https://doi.org/10.1097/01.IOP.0000056020.66654.33), indexed in Pubmed: [12644752](https://pubmed.ncbi.nlm.nih.gov/12644752/).
 8. Chan S, Dhadda AS, Swindell R. Single fraction radiotherapy for small superficial carcinoma of the skin. *Clin Oncol (R Coll Radiol)*. 2007; 19(4): 256–259, doi: [10.1016/j.clon.2007.02.004](https://doi.org/10.1016/j.clon.2007.02.004), indexed in Pubmed: [17379488](https://pubmed.ncbi.nlm.nih.gov/17379488/).
 9. Kwan W, Wilson D, Moravan V. Radiotherapy for locally advanced basal cell and squamous cell carcinomas of the skin. *Int J Radiat Oncol Biol Phys*. 2004; 60(2): 406–411, doi: [10.1016/j.ijrobp.2004.03.006](https://doi.org/10.1016/j.ijrobp.2004.03.006), indexed in Pubmed: [15380573](https://pubmed.ncbi.nlm.nih.gov/15380573/).
 10. Halperin EC, Wazer DE, Perez CA, Brady LW. *Perez & Brady's principles and practice of radiation oncology*. 7th ed. Lippincott Williams & Wilkins, New York 2018.
 11. Kuncman Ł, Kozłowski S, Pietraszek A, et al. Highly conformal CT based surface mould brachytherapy for non-melanoma skin cancers of earlobe and nose. *J Contemp Brachytherapy*. 2016; 8(3): 195–200, doi: [10.5114/jcb.2016.61066](https://doi.org/10.5114/jcb.2016.61066), indexed in Pubmed: [27504128](https://pubmed.ncbi.nlm.nih.gov/27504128/).
 12. Boman EL, Paterson DB, Pearson S, et al. Dosimetric comparison of surface mould HDR brachytherapy with VMAT. *J Med Radiat Sci*. 2018; 65(4): 311–318, doi: [10.1002/jmrs.301](https://doi.org/10.1002/jmrs.301), indexed in Pubmed: [30105776](https://pubmed.ncbi.nlm.nih.gov/30105776/).
 13. Guinot JL, Rembielak A, Perez-Calatayud J, et al. GEC ESTRO. GEC-ESTRO ACROP recommendations in skin brachytherapy. *Radiother Oncol*. 2018; 126(3): 377–385, doi: [10.1016/j.radonc.2018.01.013](https://doi.org/10.1016/j.radonc.2018.01.013), indexed in Pubmed: [29455924](https://pubmed.ncbi.nlm.nih.gov/29455924/).
 14. Rivard MJ, Coursey BM, DeWerd LA, et al. Update of AAPM Task Group No. 43 Report: A revised AAPM protocol for brachytherapy dose calculations. *Med Phys*. 2004; 31(3): 633–674, doi: [10.1118/1.1646040](https://doi.org/10.1118/1.1646040), indexed in Pubmed: [15070264](https://pubmed.ncbi.nlm.nih.gov/15070264/).
 15. Beaulieu L, Carlsson Tedgren A, Carrier JF, et al. Report of the Task Group 186 on model-based dose calculation methods in brachytherapy beyond the TG-43 formalism: current status and recommendations for clinical implementation. *Med Phys*. 2012; 39(10): 6208–6236, doi: [10.1118/1.4747264](https://doi.org/10.1118/1.4747264), indexed in Pubmed: [23039658](https://pubmed.ncbi.nlm.nih.gov/23039658/).
 16. Boman EL, Satherley TWS, Schleich N, et al. The validity of Acuros BV and TG-43 for high-dose-rate brachytherapy superficial mold treatments. *Brachytherapy*. 2017; 16(6): 1280–1288, doi: [10.1016/j.brachy.2017.08.010](https://doi.org/10.1016/j.brachy.2017.08.010), indexed in Pubmed: [28967561](https://pubmed.ncbi.nlm.nih.gov/28967561/).
 17. Fonseca G.P, Luvizotto J., Salles Coelho T. et al. Brachytherapy dose measurements in heterogenous tissues. *ISSSD 2014*: 176–88. https://inis.iaea.org/collection/NCLCollectionStore/_Public/45/089/45089765.pdf.
 18. Yu Qi Z. *Mosfet dosimetry in HDR brachytherapy and IMRT for nasopharyngeal carcinoma*. University of Wollongong, Wollongong 2010.
 19. PROTESIL normal rigid. http://www.vanninidental.com/certification/instruction_for_use/protasil_normal_rigid.pdf.
 20. Tuntipumiamorn L, Nakkrasae P, Kongkum S, et al. End-to-end test and MOSFET in vivo skin dosimetry for Ir high-dose-rate brachytherapy of chronic psoriasis. *J Contemp Brachytherapy*. 2019; 11(4): 384–391, doi: [10.5114/jcb.2019.86973](https://doi.org/10.5114/jcb.2019.86973), indexed in Pubmed: [31523241](https://pubmed.ncbi.nlm.nih.gov/31523241/).
 21. Melchert C, Soror T, Kovács G. Quality assurance during interstitial brachytherapy: dosimetry using MOSFET dosimeters. *J Contemp Brachytherapy*. 2018; 10(3): 232–237, doi: [10.5114/jcb.2018.76748](https://doi.org/10.5114/jcb.2018.76748), indexed in Pubmed: [30038643](https://pubmed.ncbi.nlm.nih.gov/30038643/).
 22. MOSFET Calibration Jig. http://www.bestmedicalcanada.com/pdf/datasheets/mosfet_calibration_jig.pdf (Dec 2019).
 23. Budrukkar A, Dasgupta A, Pandit P, et al. Clinical outcomes with high-dose-rate surface mould brachytherapy for intra-oral and skin malignancies involving head and neck region. *J Contemp Brachytherapy*. 2017; 9(3): 242–250, doi: [10.5114/jcb.2017.66773](https://doi.org/10.5114/jcb.2017.66773), indexed in Pubmed: [28725248](https://pubmed.ncbi.nlm.nih.gov/28725248/).
 24. Casey S, Awotwi-Pratt J, Bahl G. *Surface Mould Brachytherapy for Skin Cancers: The British Columbia Cancer Experience*. *Cureus*. 2019; 11(12): e6412, doi: [10.7759/cureus.6412](https://doi.org/10.7759/cureus.6412), indexed in Pubmed: [Surface Mould Brachytherapy for Skin Cancers: The British Columbia Cancer Experience](https://pubmed.ncbi.nlm.nih.gov/27504128/).
 25. Persson M, Nilsson J, Carlsson Tedgren Å. Experience of using MOSFET detectors for dose verification measurements in an end-to-end Ir brachytherapy quality assurance system. *Brachytherapy*. 2018; 17(1): 227–233, doi: [10.1016/j.brachy.2017.09.005](https://doi.org/10.1016/j.brachy.2017.09.005), indexed in Pubmed: [29110967](https://pubmed.ncbi.nlm.nih.gov/29110967/).
 26. Oare C, Wilke C, Ehler E, et al. Dose calibration of Gafchromic EBT3 film for Ir-192 brachytherapy source using 3D-printed PLA and ABS plastics. *3D Print Med*. 2019; 5(1): 3, doi: [10.1186/s41205-019-0040-4](https://doi.org/10.1186/s41205-019-0040-4), indexed in Pubmed: [30725341](https://pubmed.ncbi.nlm.nih.gov/30725341/).
 27. Bassi S, Langan B, Malone C. Dosimetry assessment of patient-specific 3D printable materials for HDR surface brachytherapy. *Phys Med*. 2019; 67: 166–175, doi: [10.1016/j.ejmp.2019.10.035](https://doi.org/10.1016/j.ejmp.2019.10.035), indexed in Pubmed: [31707143](https://pubmed.ncbi.nlm.nih.gov/31707143/).
 28. Ayobian N, Asl AS, Poorbaygi H, et al. Gafchromic film dosimetry of a new HDR 192Ir brachytherapy source. *J Appl Clin Med Phys*. 2016; 17(2): 194–205, doi: [10.1120/jacmp.v17i2.6005](https://doi.org/10.1120/jacmp.v17i2.6005), indexed in Pubmed: [27074483](https://pubmed.ncbi.nlm.nih.gov/27074483/).

29. Sinnatamby M, Nagarajan V, Kanipakam R, et al. Verification of Radiation Fluence using Stack Film in HDR Brachytherapy with Heterogeneity Algorithm. *J Clin Diagn Res.* 2018; 12: 5–10, doi: [10.7860/jcdr/2018/36733.12258](https://doi.org/10.7860/jcdr/2018/36733.12258).
30. Palmer AL, Nisbet A, Bradley D. Verification of high dose rate brachytherapy dose distributions with EBT3 Gafchromic film quality control techniques. *Phys Med Biol.* 2013; 58(3): 497–511, doi: [10.1088/0031-9155/58/3/497](https://doi.org/10.1088/0031-9155/58/3/497), indexed in Pubmed: [23306148](https://pubmed.ncbi.nlm.nih.gov/23306148/).